Coral macrobioerosion is accelerated by ocean acidification and nutrients

Thomas M. DeCarlo[1]*, Anne L. Cohen[2]*, Hannah C. Barkley[1], Quinn Cobban[3], Charles Young[4], Kathryn E. Shamberger[2†], Russell E. Brainard[4], and Yimnang Golbuu[5]

[1]Massachusetts Institute of Technology–Woods Hole Oceanographic Institution Joint Program in Oceanography/Applied Ocean Physics and Engineering, and Department of Geology and Geophysics, Woods Hole Oceanographic Institution, Woods Hole, Massachusetts 02543, USA

[2]Woods Hole Oceanographic Institution, 266 Woods Hole Road, Woods Hole, Massachusetts 02543, USA

[3]Falmouth Academy, 7 Highfield Drive, Falmouth, Massachusetts 02540, USA

[4]National Oceanic and Atmospheric Administration, Pacific Islands Fisheries Science Center, Coral Reef Ecosystem Division (NOAA CRED), 1125B Ala Moana Boulevard, Honolulu, Hawaii 96814, USA

[5]Palau International Coral Reef Center, Koror 96940, Palau

ABSTRACT

Coral reefs exist in a delicate balance between calcium carbonate ($CaCO_3$) production and $CaCO_3$ loss. Ocean acidification (OA), the CO_2-driven decline in seawater pH and $CaCO_3$ saturation state (Ω), threatens to tip this balance by decreasing calcification and increasing erosion and dissolution. While multiple CO_2 manipulation experiments show coral calcification declines under OA, the sensitivity of bioerosion to OA is less well understood. Previous work suggests that coral and coral-reef bioerosion increase with decreasing seawater Ω. However, in the surface ocean, Ω and nutrient concentrations often covary, making their relative influence difficult to resolve. Here, we exploit unique natural gradients in Ω and nutrients across the Pacific basin to quantify the impact of these factors, together and independently, on macrobioerosion rates of coral skeletons. Using an automated program to quantify macrobioerosion in three-dimensional computerized tomography (CT) scans of coral cores, we show that macrobioerosion rates of live *Porites* colonies in both low-nutrient (oligotrophic) and high-nutrient (>1 µM nitrate) waters increase significantly as Ω decreases. However, the sensitivity of macrobioerosion to Ω is ten times greater under high-nutrient conditions. Our results demonstrate that OA (decreased Ω) alone can increase coral macrobioerosion rates, but the interaction of OA with local stressors exacerbates its impact, accelerating a shift toward net $CaCO_3$ removal from coral reefs.

INTRODUCTION

Tropical coral reefs are oases of productivity that support some of the world's most biologically diverse ecosystems and important fisheries. High productivity by sessile organisms on reefs requires formation of hard calcium carbonate ($CaCO_3$) substrate in the euphotic zone, where photosynthesis can occur. This is achieved through biogenic calcification by reef organisms such as corals, coralline algae, echinoids, foraminifera, and mollusks, which, together with precipitation of abiogenic $CaCO_3$, build and cement the reef framework. Coral reef frameworks are degraded through bioerosion, the biologically mediated breakdown and dissolution of $CaCO_3$ skeletons, as well as natural dissolution and export of sand and rubble off the reef (Glynn, 1997). Today, net $CaCO_3$ accretion typically exceeds, albeit barely, net erosion and dissolution, allowing reefs to remain near the sea surface (Stearn et al., 1977; Hubbard et al., 1990).

Of mounting concern is that ocean acidification (OA), the decrease in ocean pH caused by absorption of anthropogenic CO_2, could shift this delicate balance toward a negative $CaCO_3$ budget where $CaCO_3$ loss exceeds $CaCO_3$ production. Addition of CO_2 to seawater decreases pH and lowers the $CaCO_3$ saturation state (Ω), creating a less favorable environment for $CaCO_3$ precipitation. Aragonite is the polymorph of $CaCO_3$ that corals use to build skeletons, and the $CaCO_3$ saturation state with respect to aragonite (Ω_{Arag}) is therefore a useful quantity in identifying how OA impacts the reef $CaCO_3$ budget. CO_2 laboratory manipulation experiments show that as Ω_{Arag} decreases, rates of calcification by corals and coralline algae generally decline (Kroeker et al., 2010; Chan and Connolly, 2013). Additionally, laboratory CO_2 manipulation experiments show that rates of bioerosion of coral skeleton increase with decreasing pH (Tribollet et al., 2009; Wisshak et al., 2012; Reyes-Nivia et al., 2013). The combination of declining calcification and increasing bioerosion under low pH and Ω_{Arag} implies that OA alone could drive coral reefs toward a state of net $CaCO_3$ loss. However, the impact of OA on coral reef bioerosion has not been unequivocally demonstrated outside of the laboratory because in the tropical oceans, low Ω_{Arag} generally covaries with elevated nutrients, and high nutrient concentrations can drive high rates of coral bioerosion in the absence of acidification (Risk et al., 1995; Edinger et al., 2000; Holmes et al., 2000; Tribollet and Golubic, 2005).

We exploited natural gradients in Ω_{Arag} and nutrient concentrations across the Pacific basin to investigate the independent and interactive effects of ocean acidification and nutrients on macrobioerosion rates of live colonies of the Indo-Pacific coral *Porites* spp. While macrobioerosion (>1 mm boring diameter including bivalves, worms, and sponges) of coral skeleton is a fraction of total $CaCO_3$ bioerosion on a reef (Glynn, 1997), independent studies show that macrobioerosion occurs in proportion to total bioerosion of coral rubble (Holmes et al., 2000) and experimental blocks of coral skeleton (Chazottes et al., 2002), and can thus be linked to total reef bioerosion. Macrobioerosion also affects the longevity of individual coral colonies, increasing their susceptibility to breakage and dislodgment by waves and storms (Scott and Risk, 1988; Chen et al., 2013).

MATERIALS AND METHODS

A total of 103 skeletal cores (3–7 cm diameters) were collected using underwater pneumatic and/or hydraulic drills from live *Porites* spp. coral colonies (~40–100 cm tall) that were visually healthy at 11 sampling locations within seven reef systems across the Pacific basin (Fig. 1; Table 1). Cores were drilled downwards along the axis of maximum growth from approximately the center of the colonies, to an average depth of ~35 cm. Across the Pacific basin, strong natural gradients exist in Ω_{Arag} and nutrient concentrations (Fig. 1), and in general, this pattern is supported by in situ sampling of the carbonate chemistry and dissolved inorganic nutrients of reef seawater (Table 1). Two eastern Pacific reefs (Pearl Islands and Taboga) in the Gulf of Panama are exposed to local upwelling water of low Ω_{Arag} and high nutrient concentrations (D'Croz and O'Dea, 2007; Manzello et al., 2008). In the central Pacific, Jarvis Island, Palmyra Atoll, and Kingman Reef are located near the margin of the Pacific cold tongue, where wind-driven upwelling along the equator brings water to the surface that is relatively acidic and nutrient rich compared to surrounding water. Rose Atoll and Wake Atoll are not exposed to cold-tongue waters and are characterized by

*E-mails: tdecarlo@whoi.edu; acohen@whoi.edu.

†Current address: Texas A&M University, College Station, Texas 77843, USA.

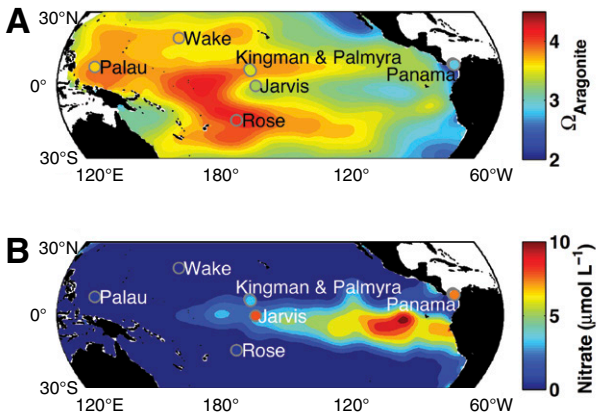

Figure 1. Study reef systems and climatological means of aragonite saturation state (Ω_{Arag}) (A) and nitrate concentration (B) in surface waters of the tropical Pacific Ocean. Ω_{Arag} is calculated using the program CO2SYS (Lewis et al., 1998) with temperature, salinity, nitrate, phosphate, and silicate climatologies from the World Ocean Atlas (Levitus, 2010), dissolved inorganic carbon climatology during the 1990s from the Global Ocean Data Analysis Project (Key et al., 2004), and total alkalinity calculated following Lee et al. (2006). Each reef system is colored by in situ seawater sample chemistry, except Wake Atoll. Palau is colored by values for Uchelbeluu.

high-Ω_{Arag}, low-nutrient conditions. On Palau, in the tropical western Pacific, a strong natural gradient in Ω_{Arag} exists across the archipelago, at persistently low nutrient concentrations (Table 1) (Shamberger et al., 2014). This reef system provides a unique opportunity to investigate the effect of low Ω_{Arag} on coral macrobioerosion in the absence of the confounding effect of elevated nutrients.

To characterize Ω_{Arag} and nutrient concentrations in reef seawater, samples were collected during multiple years, seasons, and times of day at the majority of our 11 reef locations (Table 1). Nevertheless, some degree of uncertainty remains because accurate estimates of the average Ω_{Arag} and nutritional environment over the lifetime of the coral requires sampling on all relevant time scales, including diurnal, seasonal, inter-annual, and decadal. Comparison with other in situ data sets suggests that this uncertainty is small relative to the range captured by our study sites (details are provided in the GSA Data Repository[1]).

We developed an automated computer program to quantify calcification and macrobioerosion rates in coral skeleton cores scanned by computerized tomography (CT). The program quantifies coral extension rate following the methods of Cantin et al. (2010), with modification to automatically trace the three-dimensional (3-D) growth paths of individual corallites within the core. This enables growth information to be collected from the entire 3-D core. Bulk skeletal density was determined from CT scans by comparison to coral standards, cylinders of coral skeleton whose density is calculated from mass and volume. Annual coral calcification rate (g cm^{-2} yr^{-1}) was calculated as the product of skeletal density (g cm^{-3}) and extension rate (cm yr^{-1}). The automated program is described in detail in the Data Repository.

We define "bioerosion rate" as the average rate at which $CaCO_3$ is removed from the colony over the time span represented by the core:

$$\text{bioerosion rate}\left(\text{g CaCO}_3\ \text{cm}^{-2}\ \text{yr}^{-1}\right) = \frac{(\text{volume bioeroded})(\text{skeletal density})}{(\text{coral surface area})(\text{core time span})}. \quad (1)$$

Equation 1 is equivalent to the product of percent volume bioeroded (Fig. 2) and coral calcification rate. Converting percent volume bioeroded to a mean bioerosion rate corrects potential biases caused by differences in growth rates and density amongst corals.

The data for percent volume bioeroded were fit with Ω_{Arag} as the predictor variable using a generalized additive model for location, scale, and shape with a beta inflated distribution (GAMLSS-BID; Rigby and Stasinopoulos, 2005). GAMLSS allows both the mean percent volume bioeroded and the skewness toward zero values (i.e., cores without macrobioerosion) to depend on Ω_{Arag} and nutrients. Sensitivity of macrobioerosion to Ω_{Arag} between low-nutrient (<1 μM nitrate) and high-nutrient (>1 μM nitrate) reefs was evaluated by comparing slopes of ordinary least-squares regressions fit to the reef mean macrobioerosion rates. Heteroscedasticity of the data precluded significance tests using linear regression, but did not invalidate the regression coefficients.

RESULTS AND DISCUSSION

Using only those cores collected from low-nutrient reefs spanning a natural gradient in Ω_{Arag}, we first quantified the impact of ocean acidification on macrobioerosion without the

TABLE 1. REEF LOCATIONS, MACROBIOEROSION RATES, AND SEAWATER PROPERTIES

Reef site	Latitude / longitude	Reef type	Depth (m)	Macrobioerosion rate (mg cm^{-2} yr^{-1})*	Aragonite saturation state (Ω)†§#	Nitrate (μM)†#
Nikko Bay (Palau)	7.323°N 134.494°E	Fringing / bay	1–7	17 (10, 17)	2.33 ± 0.03 (3.91)	0.2 ± 0.1 (0.1)
Risong (Palau)	7.310°N 134.477°E	Fringing / bay	1–6	11 (14, 18)	2.61 ± 0.06 (3.91)	0.4 ± 0.1 (0.1)
Airai (Palau)	7.329°N 134.557°E	Fringing	3–5	1.2 (4, 7)	3.4 ± 0.2 (3.91)	0.5 ± 0.2 (0.1)
Uchelbeluu (Palau)	7.267°N 134.521°E	Barrier	1–8	1.2 (18, 24)	3.67 ± 0.05 (3.91)	0.2 ± 0.1 (0.1)
Rose Atoll	14.545°S 168.171°W	Lagoon and fringing	4–11	0 (3, 4)	4.10 ± 0.01 (4.19)	0.4 ± 0.1 (0.1)
Wake Atoll	19.316°N 166.599°E	Fringing	14–15	0 (0, 2)	(3.71)	(0.2)
Palmyra Atoll	5.866°N 162.109°W	Fringing	12–13	0 (3, 3)	3.45 ± 0.02 (3.91)	3.1 ± 0.5 (1.3)
Kingman Reef	6.41°N 162.38°W	Lagoon and fringing	5–11	4 (7, 9)	3.42 ± 0.03 (3.91)	2.5 ± 0.8 (0.9)
Jarvis Island	0.369°S 160.008°W	Fringing	5–18	27 (4, 8)	3.29 ± 0.06 (3.44)	8 ± 2 (3)
Pearl Islands (Panama)	8.637°N 79.055°W	Fringing	5–6	65 (7, 7)	2.88 ± 0.09 (2.33)	0.27–14 (1.2)
Taboga Reef (Panama)	8.804°N 79.565°W	Fringing	3–4	68 (0, 4)	2.88 ± 0.09 (2.33)	0.27–14 (1.2)

Note: Uncertainty reported as standard error, where *n* is the number of sampling seasons and years, as indicated below for each reef location.

*First and second numbers in parentheses indicate numbers of cores used for calcification rate and macrobioerosion measurements, respectively.

†Seawater samples from Palauan reefs were collected during daylight hours in September 2011 and March 2012. Samples from Rose Atoll, Palmyra Atoll, Kingman Atoll, and Jarvis Island were collected during NOAA Pacific Reef Assessment and Monitoring Program (RAMP) cruises during daylight hours of March–April of 2006, 2008, 2010, 2012, and a September 2012 cruise to Jarvis Island. Panama Ω and nitrate are taken from Manzello et al. (2008) and D'Croz and O'Dea (2007), respectively. Parentheses indicate climatological values from World Ocean Atlas and Global Ocean Data Analysis Project (see Fig. 1).

§Determined from total alkalinity and dissolved inorganic carbon of seawater preserved with $HgCl_2$ following methods and calculations described in Shamberger et al. (2014).

#Mean absolute differences in Ω and nitrate between 12 duplicate samples were 0.035 and 0.13 μM, respectively.

[1]GSA Data Repository item 2015015, supporting text for seasonal and diurnal Ω_{Arag} variability, and Figures DR1 and DR2 (density calibration and coral calcification methods), is available online at www.geosociety.org/pubs/ft2015.htm, or on request from editing@geosociety.org or Documents Secretary, GSA, P.O. Box 9140, Boulder, CO 80301, USA.

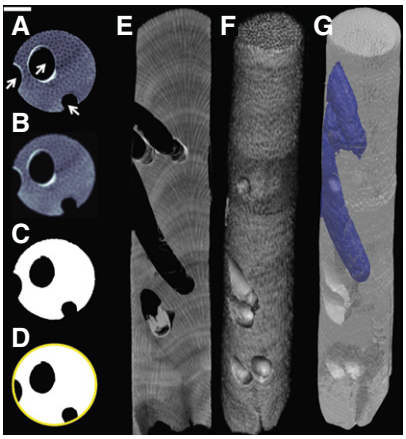

Figure 2. Macrobioerosion (by lithophagid bivalves in this particular core) in a computerized tomography scan of a *Porites* skeleton core from Panama. A–D: Axial cross-sections showing measurement of percent volume bioeroded. A shows density variability (relatively light shading indicates high density) indicating ~200 individual corallites (dark spots) and three borings (arrows). The image in A was filtered to reduce density variability of corallites in B, converted to binary (coral versus surrounding air) in C, and fit with an ellipse to identify area of borings (black regions within yellow circle) in D. E: Sagittal cross-section showing annual density banding and borings. F: Surface rendering showing outside of the core. G: Translucent surface showing borings in the center of the core (blue) that are visible in the cross-section in E but not on the outside surface of F. Scale bar in upper left is 1 cm.

confounding influence of nutrients (Fig. 3). Our results show a significant ($p < 0.05$) increase in macrobioerosion with decreasing seawater Ω_{Arag}. This result confirms that ocean acidification alone increases rates of coral macrobioerosion, consistent with laboratory experiments that show increased sponge (Wisshak et al., 2012) and micro- (Tribollet et al., 2009; Reyes-Nivia et al., 2013) bioerosion of coral skeleton under simulated OA, low-nutrient conditions. In our corals, macrobioerosion rates increase by 10 mg $CaCO_3$ cm^{-2} yr^{-1} per unit decrease of Ω_{Arag}.

Other field studies have reported high rates of bioerosion where seawater Ω_{Arag} is relatively low. For example, in the eastern tropical Pacific, high bioerosion rates (Reaka-Kudla et al., 1996) were measured on coral reefs bathed with naturally low Ω_{Arag} upwelled water (Manzello et al., 2008). Similarly, the density of macrobioeroders observed at the surface of live *Porites* colonies increased along a natural acidification gradient caused by CO_2 venting onto reefs in Papua New Guinea (Fabricius et al., 2011). Low-pH seawater caused by submarine discharge was also linked to higher incidence of bioerosion in *Porites astreoides* colonies in the Yucatan (Crook et al., 2013). In these studies, however, either low pH and low Ω_{Arag} covary with high nutrient concentrations (Manzello et al., 2008; Crook et al., 2013), or nutrient data were not reported (Fabricius et al., 2011), making it difficult to attribute increased bioerosion or bioeroder density solely to OA.

Using a second set of cores, collected from high-nutrient reefs spanning a natural gradient in Ω_{Arag}, we investigated the combined impact of ocean acidification and elevated nutrients on coral macrobioerosion rates (Fig. 3). Our results show that sensitivity of macrobioerosion rate to Ω_{Arag} increases by an order of magnitude (from 10 to 110 mg $CaCO_3$ cm^{-2} yr^{-1} per unit decrease of Ω_{Arag}) from low-nutrient reefs to high-nutrient reefs. The GAMLSS-BID analysis showed a significant effect of Ω_{Arag} on macrobioerosion within high-nutrient reefs, and a significant effect of nutrients when all reefs were included with Ω_{Arag} as a continuous predictor and nutrients as a categorical predictor. Our observation that nutrients accelerate coral bioerosion rates is consistent with that reported for live corals (Sammarco and Risk, 1990; Risk et al., 1995; Edinger et al., 2000; Holmes et al., 2000; Chen et al., 2013), coral rubble (Holmes et al., 2000), and experimental blocks of coral skeleton exposed on high-nutrient reefs (Chazottes et al., 2002; Tribollet and Golubic, 2005).

There are several potential mechanisms for coral macrobioerosion rates to increase with decreasing Ω_{Arag} and with increasing nutrients. First, relatively acidic seawater may increase the efficiency with which coral skeleton is dissolved by bioeroding organisms. For example, boring algae that infest live coral colonies, and increase their susceptibility to macrobioerosion, drive dissolution along the most soluble crystal surfaces (Kobluk and Risk, 1977). Second, nutrient enrichment may stimulate primary productivity, elevating particulate food availability and turbidity, making nutrient-rich reefs favorable environments for filter-feeding bioeroders. The role of coral skeletal density in determining sensitivity to macrobioerosion has been considered previously, with mixed results (Highsmith, 1981; Sammarco and Risk, 1990). We found no significant effect of skeletal density on macrobioerosion in the GAMLSS-BID analyses, nor did we find a relationship to water depth or reef type (Table 1).

Bioerosion is a natural process on coral reefs that supplies carbonate sediments critical to the cementation of the reef (Glynn, 1997), and may contribute to propagation of certain coral species that reproduce by fragmentation (Tunnicliffe, 1981). However, calcification must exceed bioerosion in order for reefs to grow and persist in the euphotic zone. Ocean acidification will drive a decrease in rates of calcification by corals and coralline algae, and ocean warming will exacerbate these impacts by inducing coral bleaching and mortality (Hoegh-Guldberg et al., 2007). If decreased calcification co-occurs with increased bioerosion, the $CaCO_3$ balance will shift more rapidly toward a negative $CaCO_3$ budget.

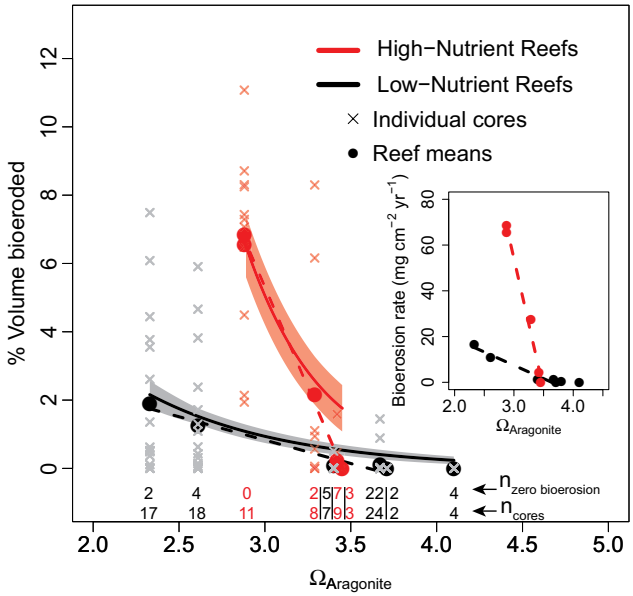

Figure 3. Relationship between macrobioerosion in skeletons of living *Porites* colonies and aragonite saturation state (Ω_{Arag}) for low-nutrient (black) and high-nutrient (red) reefs (solid lines are model fits; shading is standard error). Reef mean macrobioerosion is indicated with circles and linear fits with dashed lines. Inset shows reef mean macrobioerosion rate.

CONCLUSIONS

The results of this study show that the combination of OA (low Ω_{Arag}) and nutrient loading is ten times more effective at driving coral macrobioerosion than OA alone. Over the next century, Ω_{Arag} of reef seawater will be governed by the ocean's absorption of anthropogenic CO_2 and local and regional variability in biogeochemical processes (e.g., net photosynthesis and net calcification). Anthropogenic nutrient loading is already a major threat to coral reef ecosystems, with at least one quarter of coral reefs impacted by coastal development and watershed pollution (Burke et al., 2011). Curtailing global CO_2 emissions, the primary driver of ocean acidification, cannot be tackled at a local level. However, effective local management strategies can limit anthropogenic nutrient fluxes to coral

reefs, and are urgently needed to slow the shift to net $CaCO_3$ removal for corals, and potentially coral reef ecosystems, worldwide.

ACKNOWLEDGMENTS

We are grateful to G.P. Lohmann (Woods Hole Oceanographic Institution, WHOI), Kathryn Rose (WHOI), Jay Andrew (Palau International Coral Reef Center), Danny Merritt (National Oceanic and Atmospheric Administration, NOAA), and Edguardo Ocho (Smithsonian Institution, SI) for field assistance, and Julie Arruda (WHOI) and Darlene Ketten (WHOI) for CT scanning. Juan Mate (SI), Oris Sanjur (SI) Amanda Meyer (U.S. Fish and Wildlife Service, USFWS), Susan White (USFWS), the staff of the Palau International Coral Reef Center, and Camilo Ponton (WHOI) assisted with permitting, access to the PRIA sites, and translation of permit applications. Elizabeth Drenkard (WHOI) collected and analyzed Fall 2012 seawater samples from Jarvis Island. We thank Aline Tribollet for insightful discussion, and three anonymous reviewers whose suggestions significantly improved the manuscript. This work was supported by National Science Foundation (NSF) grant OCE 1041106 to Cohen and Shamberger, NSF grant OCE 1220529 to Cohen, The Nature Conservancy award PNA/WHOI061810 to Cohen, NSF Graduate Research Fellowships to DeCarlo and Barkley, and a WHOI-Ocean Life Institute post-doctoral fellowship to Shamberger. The NOAA Coral Reef Conservation Program provided field and logistical support for Pacific Reef Assessment and Monitoring Program research cruises. NOAA's Ocean Acidification Program provided scientific support to Brainard and Young. This paper is dedicated to the memory of Jay Andrew.

REFERENCES CITED

Burke, L.M., Reytar, K., Spalding, M., and Perry, A., 2011, Reefs at Risk Revisited: Washington, D.C., World Resources Institute, 114 p.

Cantin, N.E., Cohen, A.L., Karnauskas, K.B., Tarrant, A.M., and McCorkle, D.C., 2010, Ocean warming slows coral growth in the central Red Sea: Science, v. 329, p. 322–325, doi:10.1126/science.1190182.

Chan, N.C.S., and Connolly, S.R., 2013, Sensitivity of coral calcification to ocean acidification: A meta-analysis: Global Change Biology, v. 19, p. 282–290, doi:10.1111/gcb.12011.

Chazottes, V., Le Campion-Alsumard, T., Peyrot-Clausade, M., and Cuet, P., 2002, The effects of eutrophication-related alterations to coral reef communities on agents and rates of bioerosion (Reunion Island, Indian Ocean): Coral Reefs, v. 21, p. 375–390, doi:10.1007/s00338-002-0259-0.

Chen, T., Li, S., and Yu, K., 2013, Macrobioerosion in *Porites* corals in subtropical northern South China Sea: A limiting factor for high-latitude reef framework development: Coral Reefs, v. 32, p. 101–108, doi:10.1007/s00338-012-0946-4.

Crook, E.D., Cohen, A.L., Rebolledo-Vieyra, M., Hernandez, L., and Paytan, A., 2013, Reduced calcification and lack of acclimatization by coral colonies growing in areas of persistent natural acidification: Proceedings of the National Academy of Sciences of the United States of America, v. 110, p. 11,044–11,049, doi:10.1073/pnas.1301589110.

D'Croz, L., and O'Dea, A., 2007, Variability in upwelling along the Pacific shelf of Panama and implications for the distribution of nutrients and chlorophyll: Estuarine, Coastal and Shelf Science, v. 73, p. 325–340, doi:10.1016/j.ecss.2007.01.013.

Edinger, E.N., Limmon, G.V., Jompa, J., Widjatmoko, W., Heikoop, J.M., and Risk, M.J., 2000, Normal coral growth rates on dying reefs: Are coral growth rates good indicators of reef health?: Marine Pollution Bulletin, v. 40, p. 404–425, doi:10.1016/S0025-326X(99)00237-4.

Fabricius, K.E., Langdon, C., Uthicke, S., Humphrey, C., Noonan, S., De'ath, G., Okazaki, R., Muehllehner, N., Glas, M.S., and Lough, J.M., 2011, Losers and winners in coral reefs acclimatized to elevated carbon dioxide concentrations: Nature Climate Change, v. 1, p. 165–169, doi:10.1038/nclimate1122.

Glynn, P.W., 1997, Bioerosion and coral-reef growth: A dynamic balance, *in* Birkeland, C., ed., Life and Death of Coral Reefs: New York, Chapman and Hall, p. 68–95.

Highsmith, R.C., 1981, Coral bioerosion: Damage relative to skeletal density: American Naturalist, v. 117, p. 193–198, doi:10.1086/283698.

Hoegh-Guldberg, O., Mumby, P., Hooten, A., Steneck, R., Greenfield, P., Gomez, E., Harvell, C., Sale, P., Edwards, A., and Caldeira, K., 2007, Coral reefs under rapid climate change and ocean acidification: Science, v. 318, p. 1737–1742, doi:10.1126/science.1152509.

Holmes, K.E., Edinger, E.N., Limmon, G.V., and Risk, M.J., 2000, Bioerosion of live massive corals and branching coral rubble on Indonesian coral reefs: Marine Pollution Bulletin, v. 40, p. 606–617, doi:10.1016/S0025-326X(00)00067-9.

Hubbard, D.K., Miller, A.I., and Scaturo, D., 1990, Production and cycling of calcium carbonate in a shelf-edge reef system (St. Croix, U.S. Virgin Islands): Applications to the nature of reef systems in the fossil record: Journal of Sedimentary Research, v. 60, p. 335–360, doi:10.1306/212F9197-2B24-11D7-8648000102C1865D.

Key, R.M., Kozyr, A., Sabine, C.L., Lee, K., Wanninkhof, R., Bullister, J.L., Feely, R.A., Millero, F.J., Mordy, C., and Peng, T.H., 2004, A global ocean carbon climatology: Results from Global Data Analysis Project (GLODAP): Global Biogeochemical Cycles, v. 18, GB4031, doi:10.1029/2004GB002247.

Kobluk, D.R., and Risk, M.J., 1977, Rate and nature of infestation of a carbonate substratum by a boring alga: Journal of Experimental Marine Biology and Ecology, v. 27, p. 107–115, doi:10.1016/0022-0981(77)90131-9.

Kroeker, K., Kordas, R., Crim, R., and Singh, G., 2010, Meta-analysis reveals negative yet variable effects of ocean acidification on marine organisms: Ecology Letters, v. 13, p. 1419–1434, doi:10.1111/j.1461-0248.2010.01518.x.

Lee, K., Tong, L.T., Millero, F.J., Sabine, C.L., Dickson, A.G., Goyet, C., Park, G.H., Wanninkhof, R., Feely, R.A., and Key, R.M., 2006, Global relationships of total alkalinity with salinity and temperature in surface waters of the world's oceans: Geophysical Research Letters, v. 33, L19605, doi:10.1029/2006GL027207.

Levitus, S., 2010, NOAA Atlas NESDIS 68-71: Washington, D.C., U.S. Government Printing Office (available at http://www.nodc.noaa.gov).

Lewis, E., Wallace, D., and Allison, L., 1998, Program developed for CO_2 system calculations: Oak Ridge, Tennessee, Oak Ridge National Laboratory, Carbon Dioxide Information Analysis Center, 30 p.

Manzello, D.P., Kleypas, J.A., Budd, D.A., Eakin, C.M., Glynn, P.W., and Langdon, C., 2008, Poorly cemented coral reefs of the eastern tropical Pacific: Possible insights into reef development in a high-CO_2 world: Proceedings of the National Academy of Sciences of the United States of America, v. 105, p. 10,450–10,455, doi:10.1073/pnas.0712167105.

Reaka-Kudla, M., Feingold, J., and Glynn, W., 1996, Experimental studies of rapid bioerosion of coral reefs in the Galapagos Islands: Coral Reefs, v. 15, p. 101–107, doi:10.1007/BF01771898.

Reyes-Nivia, C., Diaz-Pulido, G., Kline, D., Guldberg, O.H., and Dove, S., 2013, Ocean acidification and warming scenarios increase microbioerosion of coral skeletons: Global Change Biology, v. 19, p. 1919–1929, doi:10.1111/gcb.12158.

Rigby, R., and Stasinopoulos, D., 2005, Generalized additive models for location, scale and shape: Journal of the Royal Statistical Society, Series C: Applied Statistics, v. 54, p. 507–554, doi:10.1111/j.1467-9876.2005.00510.x.

Risk, M., Sammarco, P., and Edinger, E., 1995, Bioerosion in *Acropora* across the continental shelf of the Great Barrier Reef: Coral Reefs, v. 14, p. 79–86, doi:10.1007/BF00303427.

Sammarco, P.P., and Risk, M.M., 1990, Large-scale patterns in internal bioerosion of *Porites*: Cross continental shelf trends on the Great Barrier Reef: Marine Ecology Progress Series, v. 59, p. 145–156, doi:10.3354/meps059145.

Scott, P., and Risk, M.J., 1988, The effect of *Lithophaga* (Bivalvia: Mytilidae) boreholes on the strength of the coral *Porites lobata*: Coral Reefs, v. 7, p. 145–151, doi:10.1007/BF00300974.

Shamberger, K.E., Cohen, A.L., Golbuu, Y., McCorkle, D.C., Lentz, S.J., and Barkley, H.C., 2014, Diverse coral communities in naturally acidified waters of a Western Pacific reef: Geophysical Research Letters, v. 41, p. 499–504, doi:10.1002/2013GL058489.

Stearn, C., Scoffin, T., and Martindale, W., 1977, Calcium carbonate budget of a fringing reef on the west coast of Barbados: Part I. Zonation and productivity: Bulletin of Marine Science, v. 27, p. 479–510.

Tribollet, A., and Golubic, S., 2005, Cross-shelf differences in the pattern and pace of bioerosion of experimental carbonate substrates exposed for 3 years on the northern Great Barrier Reef, Australia: Coral Reefs, v. 24, p. 422–434, doi:10.1007/s00338-005-0003-7.

Tribollet, A., Godinot, C., Atkinson, M., and Langdon, C., 2009, Effects of elevated pCO_2 on dissolution of coral carbonates by microbial euendoliths: Global Biogeochemical Cycles, v. 23, GB3008, doi:10.1029/2008GB003286.

Tunnicliffe, V., 1981, Breakage and propagation of the stony coral *Acropora cervicornis*: Proceedings of the National Academy of Sciences of the United States of America, v. 78, p. 2427–2431, doi:10.1073/pnas.78.4.2427.

Wisshak, M., Schönberg, C.H.L., Form, A., and Freiwald, A., 2012, Ocean acidification accelerates reef bioerosion: PLoS ONE, v. 7, e45124, doi:10.1371/journal.pone.0045124.

Manuscript received 4 August 2014
Revised manuscript received 4 October 2014
Manuscript accepted 8 October 2014

Printed in USA

GSA Data Repository 2015015

Supplemental Information for:

Coral macrobioerosion is accelerated by ocean acidification and nutrients

T.M. DeCarlo, A.L. Cohen, H.C. Barkley, Q. Cobban, C. Young, K.E. Shamberger, R.E. Brainard, and Y. Golbuu

Details of Carbonate System Chemistry Measurements

Mean Ω_{Arag} in the Gulf of Panama was calculated previously from in situ seawater samples collected during the day and night during one wet and one dry season (Manzello et al., 2008; Manzello 2010). Seawater samples from the following sites were analyzed for both alkalinity/DIC and dissolved inorganic nutrients. On Jarvis, Kingman and Palmyra, seawater samples were collected over the course of the day (9 AM to 5 PM), over multiple years (2006, 2008, 2010), primarily in springtime (March-May). Our Jarvis data include additional Fall samples (September, 2012). To assess the representativeness of our samples of average conditions, we compared pH calculated from alkalinity and DIC analyses with pH data reported by Price et al. (2012), who deployed automated, in situ SeaFet pH sensors on the same reefs over diurnal and seasonal cycles (Table DR1). Our values are within error of the Price et al. (2012) values for each reef.

On Rose Atoll, seawater samples were collected in springtime of 2006, 2008, 2010, and 2012. Mean Ω_{Arag} (4.10) calculated from in situ alkalinity and DIC is consistent with the climatology (4.19) calculated from GLODAP/World Ocean Atlas. 6 out of 103 cores were collected from Rose Atoll and Wake Atoll. Any uncertainty in our average Ω_{Arag} estimate has a small influence on our statistical model, and our significance tests and our conclusions would remain the same if data from Rose Atoll and Wake Atoll were excluded.

Within Palau, Ω_{Arag} at each sampling site was calculated from alkalinity/DIC analyses of seawater samples collected from 6 AM to 6 PM over multiple tidal cycles, seasons and years. These data are reported in Shamberger et al., (2014). To assess the representativeness of our daytime samples of the average diurnal Ω_{Arag}, we compared our Palau Ω_{Arag} values with data recently generated from seawater samples collected every two hours for 4 consecutive days in November 2013 on both a low-pH reef and a barrier (ambient pH) reef. Daytime Ω_{Arag} was not significantly different from nighttime Ω_{Arag} over this sampling period (Table DR2; K.E. Shamberger 2014 unpublished data), and our values are within error. This suggests that sampling from dawn to dusk does not bias our estimates of the mean Ω_{Arag} of our Palau sample sites.

Computerized Tomography (CT) Scans

A Siemens Volume Zoom Spiral computerized tomography (CT) scanner at Woods Hole Oceanographic Institution was used to image the cores following the methods described in Saenger et al. (2009), Cantin et al. (2010), Vásquez Bedoya et al. (2012), and Crook et al. (2013). The standard curve used to convert CT scan x-ray attenuation to density was constructed from nine, 3-cm diameter, dried *Porites* cores (Fig. DR1). Absolute bulk skeletal density of each standard, ranging from 0.809-1.537 g cm^{-3}, was calculated as the quotient of measured core mass and volume.

Automated Analysis of CT Scan Data to Quantify Coral Skeletal Parameters (Extension, Density, Calcification)

Calcification rate (g cm^{-2} yr^{-1}) was calculated as the product of extension of the coral colony surface during one year (cm yr^{-1}) and density of skeleton over the year's extension (g cm^{-3}) (Barnes and Lough 1993).

Corallites were identified in each image by finding local density minima, which are the porous centers of calices surrounded by dense thecal walls. Images were first filtered with a 2-dimensional Gaussian filter (standard deviation 0.29 mm and clipped at 0.97 mm), which resulted in one local density minima per corallite (Fig. DR2). A Euclidian-distance nearest neighbors approach was used to assign each voxel within the core to the nearest corallite. The mean density of all voxels in one image assigned to a given corallite was taken as the corallite density in that image. Finding the corallite in one image nearest to the location of a corallite in the previous image connected the corallites throughout the core.

Annual density bands were identified by visual inspection of slabs digitally cut along the vertical growth axis of the cores (Fig. DR2). Local density minima (annual bands) were identified in several locations in each slab and repeated in 4 slabs throughout the core. Low-density bands were mapped in 3-dimensions by interpolating between the coordinates where the bands were marked.

Corallite density tracks were used to objectively define the locations of annual density bands. For each identified band, all corallites passing through the band were searched for local density minima within 1 mm of the identified band location. If a density minimum was found, the annual band at the location of the given corallite was shifted to match the density minimum. After making adjustments for all corallites passing through a band, the new coordinates of the band were interpolated to map the band in 3-dimensions. Bands were smoothed by a 2-dimensional Gaussian filter (standard deviation 0.97 mm and clipped at 0.97 mm).

For each year's growth (region between 2 low-density bands), all corallites were identified that extended in the core throughout the full year. A vector was fit to the 3-dimensional coordinates every 2 mm of vertical growth with the origin set to the first corallite coordinate, the vector direction determined by singular value decomposition and

the magnitude (length) determined by Euclidian distance. The sum of lengths of all vectors fit on a corallite's path between annual bands was taken as the annual extension rate of that corallite. Calcification rate was determined for each corallite as the product of annual extension and density, and all corallite calcification rates were averaged to determine the annual whole-core calcification rate. All image analyses were conducted with MATLAB 2012a.

REFERENCES CITED

Barnes, D., and Lough, J., 1993, On the nature and causes of density banding in massive coral skeletons: Journal of experimental marine biology and ecology, v. 167, no. 1, p. 91-108, doi:10.1016/0022-0981(93)90186-R.

Cantin, N.E., Cohen, A.L., Karnauskas, K.B., Tarrant, A.M., and McCorkle, D.C., 2010, Ocean warming slows coral growth in the central Red Sea: Science, v. 329, no. 5989, p. 322-325, doi:10.1126/science.1190182.

Crook, E.D., Cohen, A.L., Rebolledo-Vieyra, M., Hernandez, L., and Paytan, A., 2013, Reduced calcification and lack of acclimatization by coral colonies growing in areas of persistent natural acidification: Proceedings of the National Academy of Sciences of the United States of America, v. 110, no. 27, p. 11044–11049, doi:10.1073/pnas.1301589110.

Manzello, D. P., 2010, Ocean acidification hot spots: Spatiotemporal dynamics of the seawater CO_2 system of eastern Pacific coral reefs: Limnology and Oceanography, v. 55, no. 1, p. 239-248, doi:10.4319/lo.2010.55.1.0239.

Manzello, D.P., Kleypas, J.A., Budd, D.A., Eakin, C.M., Glynn, P.W., and Langdon, C., 2008, Poorly cemented coral reefs of the eastern tropical Pacific: Possible insights into reef development in a high-CO_2 world: Proceedings of the National Academy of Sciences of the United States of America, v. 105, no. 30, p. 10450–10455, doi:10.1073/pnas.0712167105.

Price, N. N., Martz, T. R., Brainard, R. E., and Smith, J. E., 2012, Diel variability in seawater pH relates to calcification and benthic community structure on coral reefs: PLoS One, v. 7, no. 8, p. e43843, doi:10.1371/journal.pone.0043843.

Saenger, C., Cohen, A. L., Oppo, D. W., Halley, R. B., and Carilli, J. E., 2009, Surface-temperature trends and variability in the low-latitude North Atlantic since 1552: Nature Geoscience, v. 2, no. 7, p. 492-495, doi:10.1038/ngeo552.

Shamberger, K.E., Cohen, A.L., Golbuu, Y., McCorkle, D.C., Lentz, S.J., and Barkley, H.C., 2014, Diverse coral communities in naturally acidified waters of a Western Pacific reef: Geophysical Research Letters, v. 41, no. 2, p. 499–504, doi:10.1002/2013GL058489.

Vásquez□Bedoya, L. F., Cohen, A. L., Oppo, D. W., and Blanchon, P., 2012, Corals record persistent multidecadal SST variability in the Atlantic Warm Pool since 1775 AD: Paleoceanography, v. 27, no. 3, p. PA3231, doi:10.1029/2012PA002313.

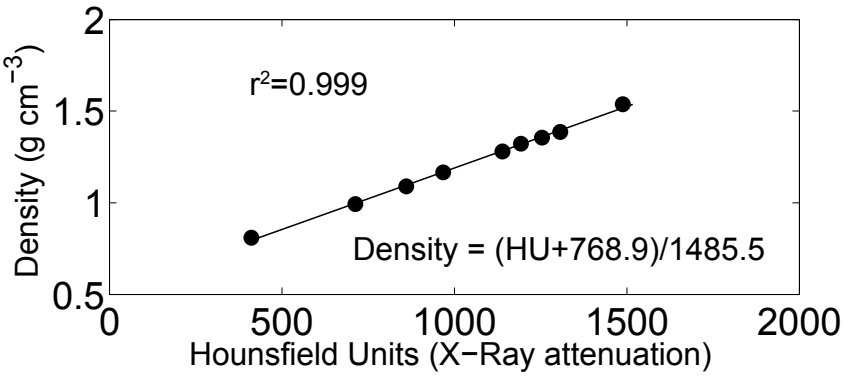

Figure DR1. Standard curve used to convert CT attenuation (Hounsfield Units) to bulk coral skeletal density (g cm^{-3}).

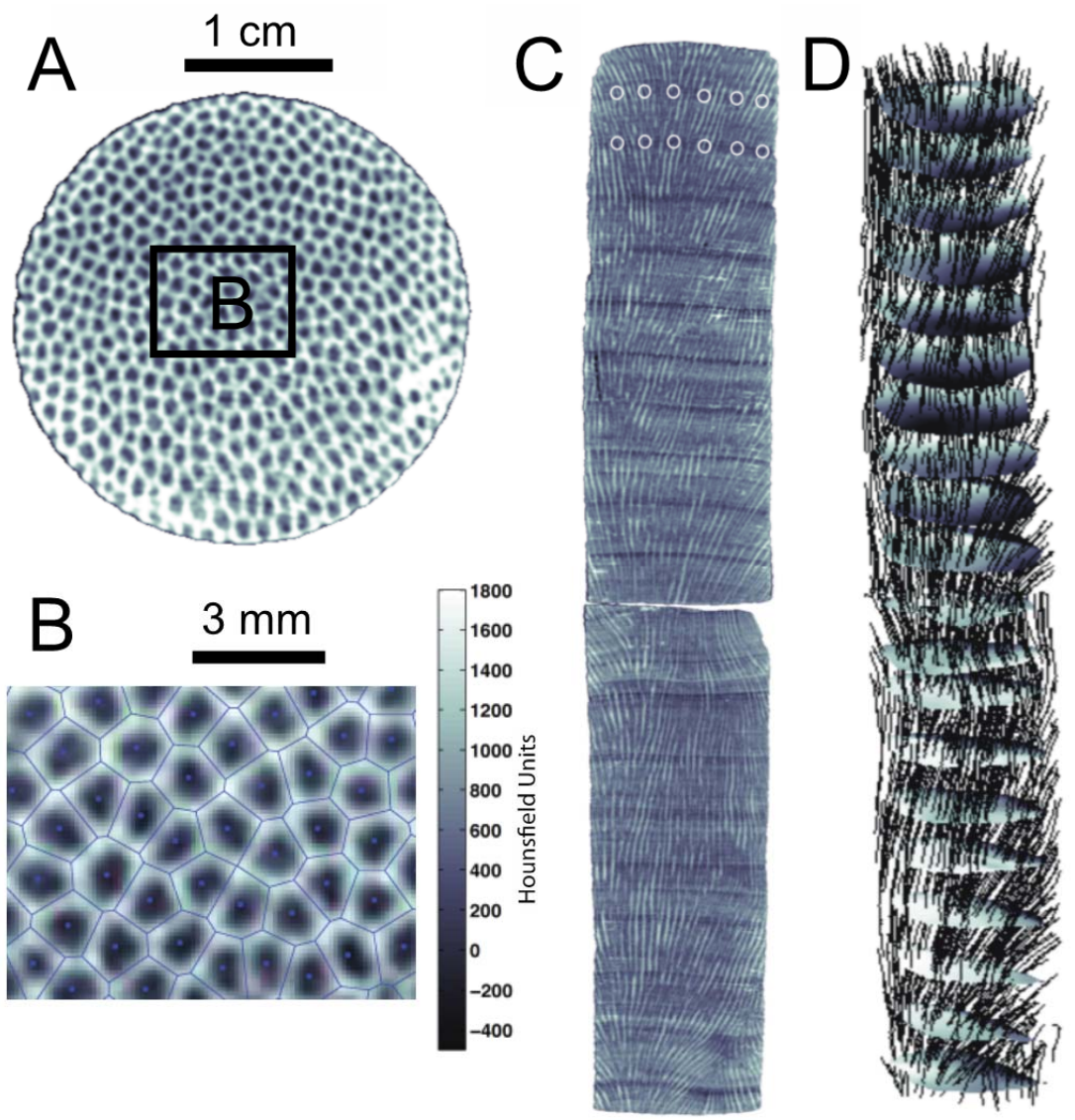

Figure DR2. Calcification rate analysis of a CT scan of a Porites core. A: Axial cross-section of the core that shows corallites (dark regions, low density) surrounded by skeletal walls (white, high density). B: Blue dots indicate corallites that are identified by local density minima. Blue lines show a Voronoi diagram drawn around the corallites. C: Digital slab cut in the sagittal plane. Near-vertical light and dark streaks are paths of individual corallites through the core. Horizontal dark (low density) bands are annual growth bands. The first two low-density bands are identified in the figure, as indicated by the white circles. D: 3-dimensional reconstruction of annual banding and corallite paths. Horizontal surfaces are the mapped and interpolated annual low-density bands, which are shaded to aid visualization of 3-dimensional shape. Black lines indicate paths of individual corallites traced through the core. For clarity, the image is viewed from an oblique angle looking slightly downward, and only 20% of all corallite paths are plotted. Scale bar is 1 cm and the core is 30 cm in height.

TABLE DR1. PH MEASURED ON CENTRAL PACIFIC REEFS

Reef Site	Our pH	Price et al. (2012) pH
Jarvis Island	7.98 ± 0.02	8.005 ± 0.013
Palmyra Atoll S forereef	8.007 ± 0.011	7.995 ± 0.012
Kingman Reef	8.004 ± 0.012	8.025 ± 0.009

TABLE DR2. DIURNAL VARIABILITY OF ARAGONITE SATURATION STATE (Ω) IN PALAU

Reef Site	Daytime Ω ± 1σ	Nighttime Ω ± 1σ	Average Diurnal Ω ± 1σ
Low pH bay reef	2.77 ± 0.05	2.74 ± 0.20	2.75 ± 0.22
Barrier reef	3.72 ± 0.27	3.57 ± 0.27	3.66 ± 0.28